

Magnetic Ferroelectrics Bi, Pb-3d transition metal perovskites

Masaki Azuma, Seiji Niitaka*, Alexei Belik†, Shintaro Ishiwata‡, Takashi Saito, Kazuhide Takata, Ikuya Yamada, Yuichi Shimakawa and Mikio Takano

Institute for Chemical Research, Kyoto University, Uji, Kyoto-fu 611-0011

Fax: +81-774-38-3125, e-mail: masaki@scl.kyoto-u.ac.jp

* Magnetic Materials Laboratory, RIKEN (Institute of Physical and Chemical Research), Wako 351-0198, Japan

† International Center for Young Scientists, National Institute for Materials Science, Tsukuba, 305-0044, Japan

‡ Department of Applied Physics, Waseda University, Shinjuku, Tokyo 169-8555, Japan.

Crystal structures and magnetic, electric properties of Bi, Pb-3d transition metal perovskites stabilized by high-pressure synthesis were investigated. BiCrO₃ was found to be an antiferromagnetic ferroelectric with BiMnO₃ structure. BiCoO₃ and PbVO₃ are isotypic with PbTiO₃. Spontaneous polarizations of ~ 100 μC/cm² are expected from the atomic displacements. BiNiO₃ is an antiferromagnetic insulator with oxidation state of Bi³⁺_{1/2}Bi⁵⁺_{1/2}Ni²⁺O₃. Based on these results, a new ferromagnetic ferroelectric double perovskite Bi₂NiMnO₆ was designed and was synthesized. In this compound, Ni²⁺ (*t*_{2g}⁶*e*_g²) and Mn⁴⁺ (*t*_{2g}³) ions are ordered in a NaCl configuration leading to a ferromagnetic interaction. As a result, ferroelectric and ferromagnetic transitions were observed at 485 and 140 K, respectively.

Key words: magnetic ferroelectric, transition metal oxides, perovskites, high-pressure synthesis

1. INTRODUCTION

A compound where magnetic and ferroelectric orders coexist is potentially of great use. It records digital data as combinations of electric and magnetic signals, so the capacity of the magnetic ferroelectric memory device will be $4n$ instead of $2n$ (n : cell number). If the coupling between magnetic and dielectric properties is strong enough to switch the direction of magnetization by application of an electric field, the thermal power of a magnetic memory will be drastically reduced. Discovery of anomalously large interplay between ferroelectricity and magnetism in TbMnO₃¹ and TbMn₂O₅² has accelerated such interest. Despite their usefulness, magnetic ferroelectrics are rare in nature and most of them are antiferromagnets with small responses to an external magnetic field. A classical way to obtain a magnetic ferroelectric is to locate Bi³⁺ or Pb²⁺ ion and a magnetic transition metal ion on *A* and *B* sites of a ABO₃ perovskite structure, respectively. The 6s² lone pair of Bi (Pb) ion and the strong covalent character of Bi(Pb)-O bonds stabilize a noncentrosymmetric distorted structure^{3,4} as illustrated in Fig. 1(a). Consequently, spontaneous polarization of PbTiO₃ is about 3 times as large as that of BaTiO₃. BiFeO₃ is the only Bi,Pb-3d transition metal perovskite which can be prepared at ambient pressure. It is a well known antiferromagnetic ($T_N = 643$ K) ferroelectric ($T_{CE} = 1103$ K)⁵ with a small spontaneous polarization of 5 μC/cm² in the <111> direction of the rhombohedral unit cell. Large

polarization and weak ferromagnetism due to a spin canting were recently reported in an epitaxial thin film of a tetragonal PbTiO₃-type structure and stimulated many of the following works.⁶ High-pressure (HP) synthesis is a powerful tool to stabilize such distorted structures. HP syntheses of Bi,Pb-3d transition metal perovskites were reported in the late 1960's, but their crystal structures and physical properties were not studied well.⁷⁻⁹ Among them, BiMnO₃¹⁰⁻¹² has recently been found to be ferromagnetic ($T_{CM} = 110$ K) ferroelectric ($T_{CE} = 760$ K) and attracts much attention. We have studied other Bi, Pb-3d transition metal perovskites, BiCrO₃¹³, BiCoO₃^{14,15}, BiNiO₃¹⁶ and PbVO₃¹⁷. Based on these results, new ferromagnetic ferroelectric compound Bi₂NiMnO₆ was designed and synthesized¹⁸. In this manuscript, the relations between the structures and the properties of these compounds will be discussed.

2. EXPERIMENT

Polycrystalline samples were prepared by high-pressure synthesis at 3-6 GPa. Gold capsules charged with starting oxides were compressed in a cubic anvil type apparatus and then heated. Crystal structures were determined by Rietveld analyses of synchrotron X-ray and neutron powder diffraction data collected at BL02B2 of SPring-8 and Vega at KENS, KEEK, respectively. A program RIERAN-2000¹⁹ was used for the analyses. Magnetic and electric measurements were performed with a Quantum Design SQUID Magnetometer (MPMS) and a Physical Property Measurement System (PPMS), respectively. Dielectric constants were measured using a LCR meter (Agilent 4284A)

3. RESULTS AND DISCUSSIONS

3.1 BiCrO₃ and BiMnO₃

BiCrO₃ was prepared from Bi₂O₃ + Cr₂O₃ at 4 GPa, 973 ~ 1273 K¹³. Figure 2 shows the synchrotron X-ray powder diffraction (SXRD) data taken at 300 and 500 K.

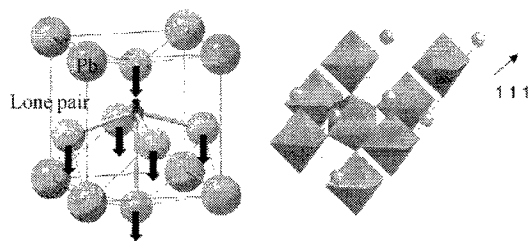


Fig. 1. Crystal structures of PbTiO₃ (a) and BiFeO₃ (b).

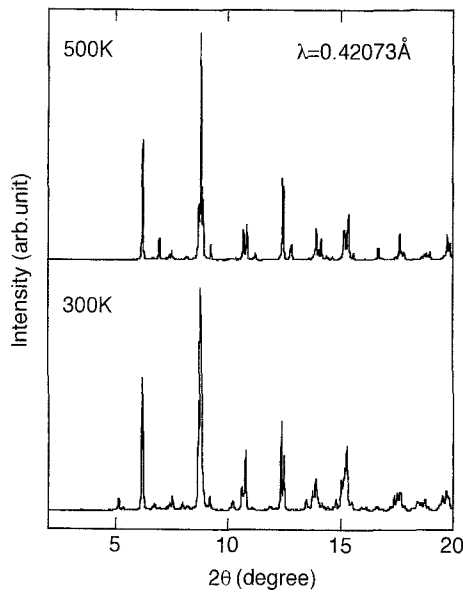


Fig. 2. Synchrotron X-ray powder diffraction pattern of BiCrO₃ at 300 and 500 K.

The room temperature structure shown in Fig. 3(a) was found to be basically the same as that of BiMnO₃, monoclinic with $a = 9.471 \text{ \AA}$, $b = 5.486 \text{ \AA}$, $c = 9.593 \text{ \AA}$ and $\beta = 108.58^\circ$. The space group $C2$ allows the electric polarization of $\sim 20 \mu\text{C}/\text{cm}^2$ along the b axis. The crystal structure changes to orthorhombic GdFeO₃ type ($Pnma$) shown in Fig. 3(b) at 440 K. This transition from acentric to centric structures corresponds to a ferroelectric transition. Accordingly, a peak was

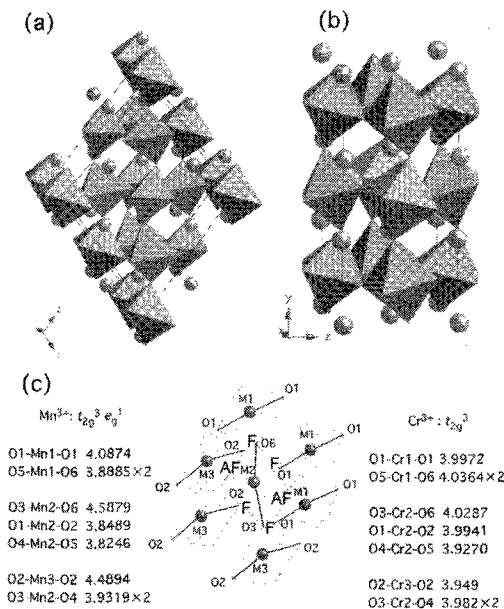


Fig. 3. Crystal structures of BiMnO₃ and BiCrO₃ at room temperature (a) and high temperature (b). Linkage of MnO₆ and CrO₆ octahedra is shown in (c)

observed in the temperature dependence of dielectric constant.

BiCrO₃ is an antiferromagnet with $T_N = 116 \text{ K}$ ¹³ while BiMnO₃ is a ferromagnet with $T_{CM} = 110 \text{ K}$ despite the structural similarity. This contrast owes to the difference in the electric configurations of Cr³⁺ (t_{2g}^3) and Mn³⁺ ($t_{2g}^3 e_g^1$). Figure 3(c) shows the linkage of Mn(Cr)O₆ octahedra of BiMnO₃ and BiCrO₃. MnO₆ octahedra of BiMnO₃ are elongated in one direction because of the Jahn-Teller distortion. Only one of the 2 e_g orbitals (d_{z^2}) is occupied with an electron. In the figure, the thick lines stand for the long O-Mn-O bonds. These correspond to Jahn-Teller axes, in other words, the direction of the occupied d_{z^2} orbitals. There is a 3 dimensional order of the d_{z^2} orbitals. As a result, no linear Mn d_{z^2} - O - Mn d_{z^2} bond mediating strong antiferromagnetic interaction exists in BiMnO₃. The symbols "F" stand for the orthogonal arrangements of d_{z^2} orbitals. Ferromagnetic interaction is expected in such configuration. This is the origin of the ferromagnetism of BiMnO₃.¹¹ On the other hand, CrO₆ octahedra of BiCrO₃ are regular, *i.e.*, there is no elongated O-Cr-O bond²⁰. This clearly indicates the absence of Jahn-Teller distortion in BiCrO₃ reflecting the t_{2g}^3 electric configuration. BiCrO₃ is thus an antiferromagnet ferroelectric with $T_N = 116 \text{ K}$ and $T_{CE} = 440 \text{ K}$.

3.2 PbVO₃ and BiCoO₃

PbTiO₃ is the only simple perovskite oxide with the composition PbMO₃ (M is a transition metal) which can be prepared at ambient pressure. It is known that two other members, PbCrO₃ and PbMnO₃, can be obtained by high-pressure synthesis. The former was reported to have a simple cubic perovskite structure, and the latter has a 6H hexagonal perovskite-type structure, the same as the high temperature phase of BaTiO₃.

A new perovskite-type oxide PbVO₃ with V⁴⁺ (spin-1/2) was prepared from the mixture of PbO, V₂O₃ and V₂O₅ at 6 GPa and 1273 K.¹⁵ PbVO₃ was found to be isotopic with PbTiO₃, with lattice parameters of $a = 3.80391(5)$ and $c = 4.67680(8)$ ^{17,21}. The tetragonal

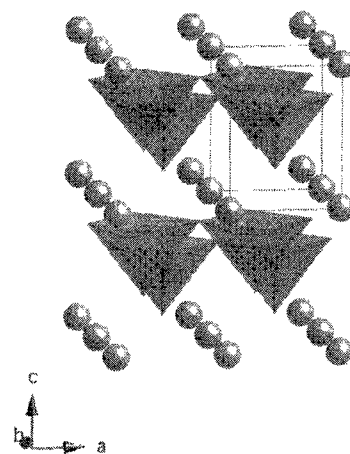


Fig. 4 Crystal Structure of PbVO₃.

distortion, $c/a = 1.229$ in PbVO_3 is the largest among the reported PbTiO_3 -type materials. An estimation assuming a point charge model indicated a large polarization of $101 \mu\text{C}/\text{cm}^2$. This large polarization prevents us from the observation of P-E hysteresis curve on a polycrystalline specimen. Also, the transition to cubic structure corresponding to the ferroelectric transition is not observed below 600 K. Above this temperature, PbVO_3 was oxidized to $\text{Pb}_2\text{V}_2\text{O}_7$. The structural transition was observed at high pressure. Figure 5 shows the powder diffraction pattern of PbVO_3 at elevated pressures taken at BL14B1 of SPring-8. 101 and 110 peaks of the tetragonal phase merge at 3.8 GPa, indicating the transition to the cubic phase. An insulator to metallic transition was also observed at the same pressure.

It should be noted that BiCoO_3 also has tetragonal PbTiO_3 type structure. It is an antiferromagnet with $T_N = 470 \text{ K}$.^{14,15}

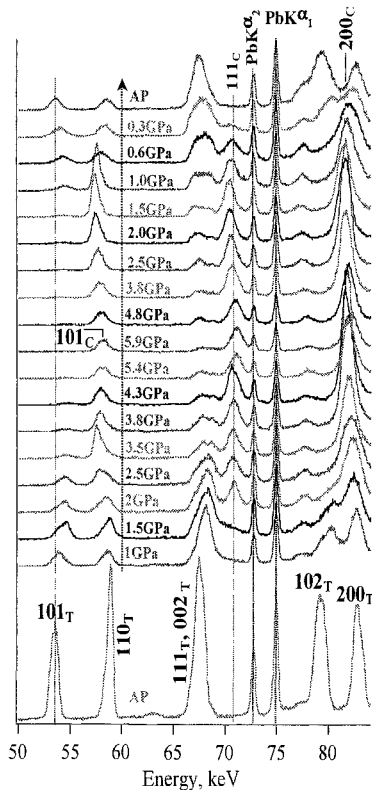


Fig. 5. SXRD patterns of PbVO_3 at high pressures and at room temperature.

3.3 BiNiO_3

Ni(III) perovskite RNiO_3 ($R = \text{lanthanides, Y and Tl}$) changes the properties depending on the ionic size of R ion. The charge disproportionation ($2\text{Ni}^{3+} \rightarrow \text{Ni}^{(3+\delta)+} + \text{Ni}^{(3-\delta)+}$) associated with orthorhombic to monoclinic distortion has been observed for RNiO_3 with small lanthanides ($R = \text{Ho to Lu}$). On the other hand, LaNiO_3 keeps a metallic conductivity and rhombohedral structure in the whole temperature range. In this context, BiNiO_3 is expected to be cubic and metallic because the Bi^{3+} ionic size is even larger than La^{3+} .

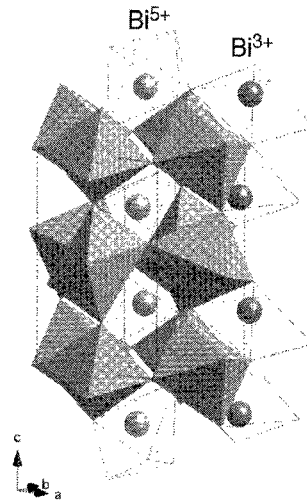


Fig. 6. Crystal Structure of BiNiO_3 .

Polycrystalline sample was synthesized at 6 GPa in an oxidizing atmosphere generated by the decomposition of KClO_4 .¹⁶ The refined structure is a distorted GdFeO_3 type with a triclinic unit cell (P-1, $a = 5.38512(8) \text{ \AA}$, $b = 5.64972(8) \text{ \AA}$, $c = 7.70768(12) \text{ \AA}$, $\alpha = 91.9529(10)^\circ$, $\beta = 89.8096(9)^\circ$, $\gamma = 91.5411(9)^\circ$). There are 2 Bi sites and 4 Ni sites in the unit cell. The bond-valence calculation²² indicated the disproportionation of Bi into Bi^{3+} and Bi^{5+} and the consequent reduction of the Ni ion to 2+ oxidation state. BiNiO_3 is $\text{Bi}^{3+}_{1/2}\text{Bi}^{5+}_{1/2}\text{Ni}^{2+}\text{O}_3$ rather than $\text{Bi}^{3+}\text{Ni}^{3+}\text{O}_3$.

Contrarily to our expectation, the system is an antiferromagnetic insulator with localized $S=1$ characterized by Ni^{2+} . However, partial substitution of La^{3+} for Bi induced the metallic conductivity²³. Figure 5 shows the temperature dependence of the resistivity of $\text{Bi}_{1-x}\text{La}_x\text{NiO}_3$. Samples with $x = 0.075, 0.1$ and 0.2 exhibits temperature-induced insulator to metal

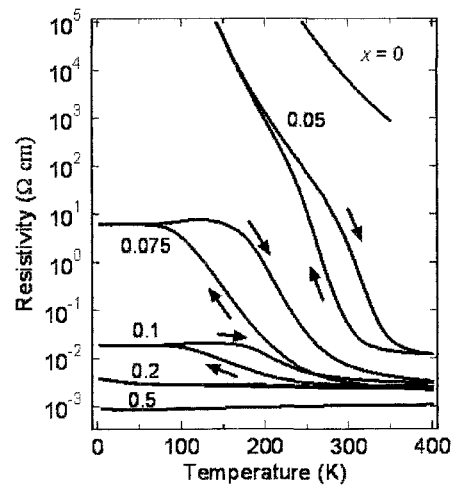


Fig. 7 Temperature dependence of the resistivity of $\text{Bi}_{1-x}\text{La}_x\text{NiO}_3$.

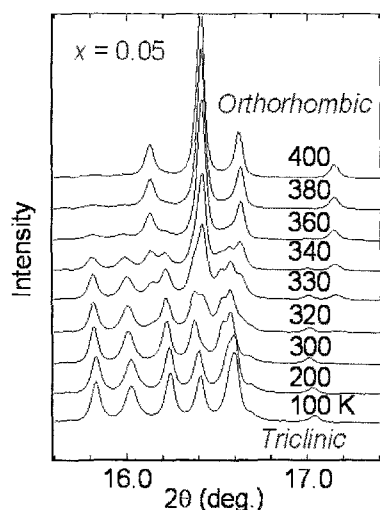


Fig. 8. SXR D patterns of $\text{Bi}_{0.95}\text{La}_{0.05}\text{NiO}_3$ at various temperatures.

transition. Structural transitions from triclinic to orthorhombic one was also observed at the same temperature as shown in fig. 8 for $x = 0.05$ sample. 5 main peaks of SXR D pattern characteristic for the triclinic phase merged into 3. This indicates the melting of the A-site disproportionation because both Bi and Ni have single crystallographic sites in the orthorhombic GdFeO_3 type structure. Photoemission study has revealed that the oxidation state of the metallic phase is $\text{Bi}^{4+}_{1-x}\text{La}^{3+}_x\text{Ni}^{2+x}\text{O}_3$ ²⁴. This structural change associated with insulator to metal transition was induced by the application of the pressure of 4 GPa as well.

3.4 Designed Ferromagnetic Ferroelectric $\text{Bi}_2\text{NiMnO}_6$

As shown above, BiMnO_3 is the only ferromagnet among Bi,Pb-3d transition metal perovskites. The ferromagnetism of this compound results from a particular orbital order as illustrated in Fig. 9(a). According to the Kanamori-Goodenough rules, a ferromagnetic insulator can also be expected for the configuration shown in Fig. 8(b). This can be realized by distributing 2 kinds of transition metal ions with and without e_g electrons in a rock-salt configuration. $\text{Bi}_2\text{NiMnO}_6$ is thus expected to be a ferromagnetic ferroelectric.

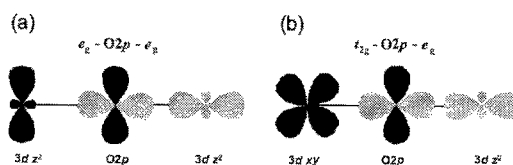


Fig. 9. Arrangements of d orbitals where ferromagnetic interactions are expected.

Bulk sample of $\text{Bi}_2\text{NiMnO}_6$ was prepared from a stoichiometric mixture of Bi_2O_3 , NiO and MnO_2 at 6 GPa and 1073 K.¹⁸ Then it was slowly cooled to the

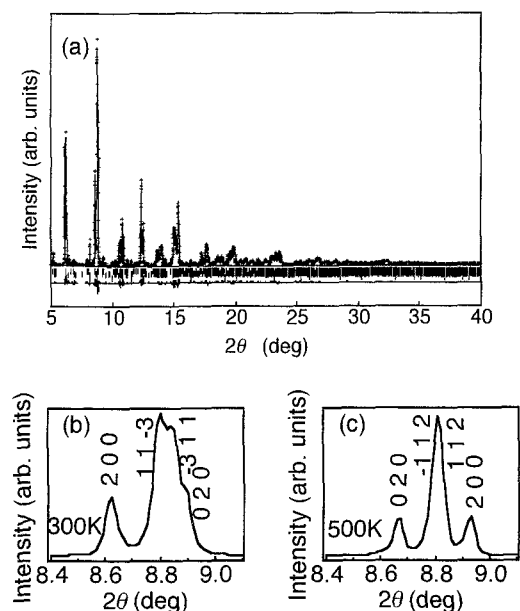


Fig. 10 Synchrotron X-ray powder diffraction pattern for $\text{Bi}_2\text{NiMnO}_6$ at 300 K (a). Magnified view of the patterns taken at 300 K (b) and 500 K (c).

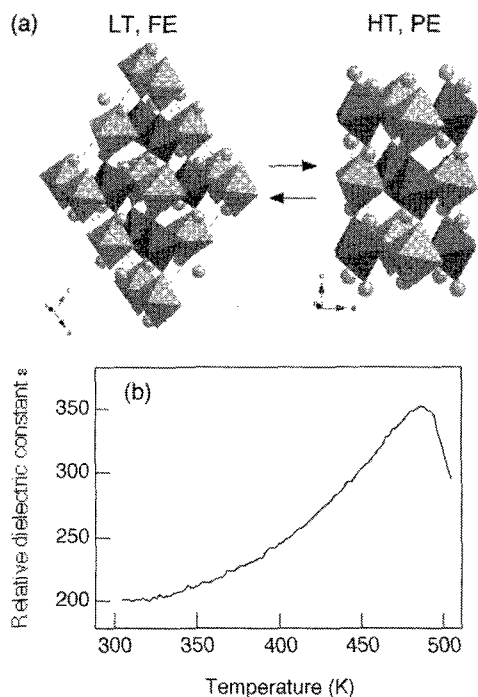


Fig. 11. Crystal structures of the room temperature (ferroelectric) and high-temperature (paraelectric) phases of $\text{Bi}_2\text{NiMnO}_6$ (a). Temperature dependence of relative dielectric constant (b).

room temperature in 4-50 hours before releasing the pressure. Fig. 10 shows the synchrotron X-ray powder diffraction pattern taken at room temperature. The diffraction peaks could be indexed with a monoclinic unit cell of $a = 9.4646(4)$ Å, $b = 5.4230(2)$ Å, $c = 9.5431(4)$ Å and $\beta = 107.823(2)^\circ$. Since the unit cell

was close to those of BiMnO_3 and BiCrO_3 , a Rietveld structure refinement was performed assuming a BiMnO_3 -type structure as an initial model. There are 3 transition metal sites, M1, M2 and M3 with multiplicities of 2, 4 and 2 in this structure. At the initial stage of the refinement, Ni^{2+} and Mn^{4+} were randomly distributed over these 3 sites. It was found that the M-O bond lengths were considerably shorter for M2 site than M1 and M3 sites, so small Mn^{4+} ion was assigned to M2 site, and large Ni^{2+} ions were assigned to M1 and M3 at the final stage. Bond valence sums calculated from the refined structural parameters were 2.14, 2.17 and 3.62 for Ni1, Ni2 and Mn ions, confirming the validity of this model. The determined crystal structure is shown in Fig. 11 (a). Large Ni^{2+} octahedra and small Mn^{4+} octahedra are ordered in a rock-salt configuration as we expected. The NiO_6 and MnO_6 octahedra of $\text{Bi}_2\text{NiMnO}_6$ are rather isotropic reflecting the absence of a Jahn-Teller (J-T) distortion. This is in contrast with BiMnO_3 where the O1-Mn1-O1, O3-Mn2-O6 and O2-Mn3-O2 bonds are longer than other O-Mn-O bonds by more than 10 % reflecting the electronic configuration of Mn^{3+} ions, $t_{2g}^3 e_g^1$ ($S=2$), and the ordering of the occupied e_g orbitals.^{10,11} The absence of the J-T distortion in NiO_6 and MnO_6 octahedra also supports the Ni^{2+} ($t_{2g}^6 e_g^2$) and Mn^{4+} (t_{2g}^3) oxidation states in $\text{Bi}_2\text{NiMnO}_6$.

The C_2 symmetry of this compound allows a spontaneous polarization along the b axis, and a calculation assuming a point-charge model with the above structural parameters gave a polarization of $\sim 20 \mu\text{C}/\text{cm}^2$. The ferroelectric transition was observed by a dielectric constant measurement and also by a structural study. Figure 11(b) shows the temperature dependence of the relative dielectric constant. A peak was found at 485 K suggesting the ferroelectric transition. Correspondingly the crystal structure changed above T_{CE} . Figure 10 (b) and (c) show portions of powder X-ray diffraction patterns. The pattern at 500 K was indexed with a monoclinic cell of $a = 5.4041(2) \text{ \AA}$, $b = 5.5669(1)$

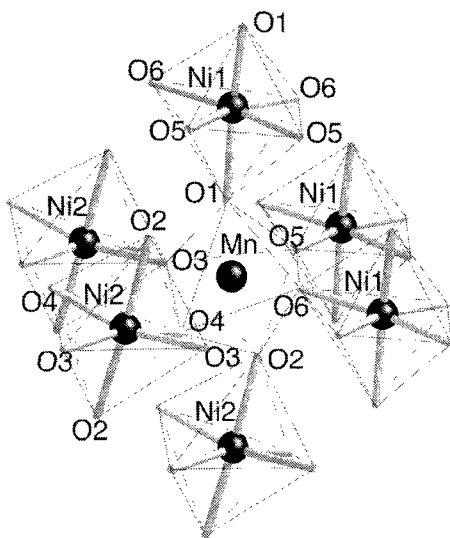


Fig. 12. Linkage of NiO_6 and MnO_6 octahedra of $\text{Bi}_2\text{NiMnO}_6$.

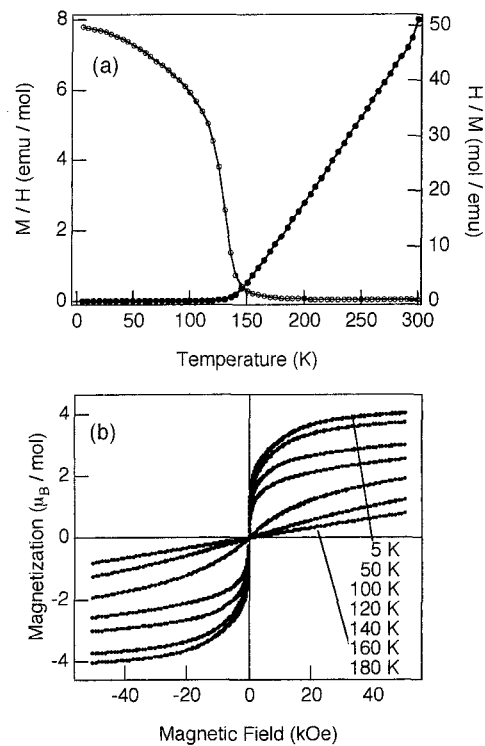


Fig. 13. Temperature dependences of magnetic susceptibility and inverse susceptibility of $\text{Bi}_2\text{NiMnO}_6$ (a). Magnetization of at various temperatures (b).

Å , $c = 7.7338(2) \text{ \AA}$ and $\beta = 90.184(2)^\circ$. This $\sqrt{2}a \times \sqrt{2}a \times 2a$ monoclinic supercell of a cubic perovskite is the same as those of the high temperature (paraelectric) phases of BiMnO_3 and BiCrO_3 , orthorhombic GdFeO_3 type structure. However, there is only one Mn (Cr) site in GdFeO_3 structure. The monoclinic distortion is the sign of the ordering of Ni^{2+} and Mn^{4+} because $\text{La}_2\text{NiMnO}_6$ ²⁵ where Ni^{2+} and Mn^{4+} are ordered in a rock-salt type configuration has the same monoclinic unit cell (space group $P2_1/n$). This distorted GdFeO_3 type structure as illustrated in Fig. 11(a) is the same as that of the low temperature (charge disproportionated) phase of RNiO_3 . Rietveld refinement confirmed that the HT phase of $\text{Bi}_2\text{NiMnO}_6$ had the same centrosymmetric structure as $\text{La}_2\text{NiMnO}_6$. This phase transition from a centric GdFeO_3 type to acentric structure with C_2 symmetry is the same as those of BiCrO_3 and BiMnO_3 . Therefore it is reasonable to regard $\text{Bi}_2\text{NiMnO}_6$ as a ferroelectric compound with $T_{\text{CE}} = 485 \text{ K}$. As shown in Fig. 12, the MnO_6 octahedron is surrounded by 6 NiO_6 octahedra and *vice versa*, so the magnetic exchange path is $-\text{Ni}^{2+}-\text{O}-\text{Mn}^{4+}-\text{O}-\text{Ni}^{2+}$. Since a Ni^{2+} ion has the e_g^2 configuration while Mn^{4+} has no e_g electron, a ferromagnetic interaction is expected between the adjacent spins. Figure 13(a) shows the temperature dependence of the magnetic susceptibility measured on cooling in an external field of 100 Oe. The data exhibit a sharp increase at 140 K indicating the ferromagnetic transition. As seen in the inverse $\chi-T$ plot in the same figure, the Weiss constant was 140 K, also confirming the ferromagnetic interactions between Ni and Mn spins. The magnetization measured at 5 K was $4.1 \mu_B$ at 5 T as

shown in Fig. 13(b). This value is close to $5 \mu_B$ expected from Ni^{2+} ($S = 1$) and Mn^{4+} ($S = 3/2$) but is still smaller. This is probably due to a small antisite disorder of Ni^{2+} and Mn^{4+} ions. The resulting Ni-O-Ni and Mn-O-Mn magnetic paths give antiferromagnetic interactions, and thus reduce the saturated magnetization. The quenching from 1073 K after the HP synthesis before releasing the pressure resulted in the random mixing of Mn and Ni and a substantial decrease of the ordered magnetic moment was observed. It should be emphasized that our material design of Bi or Pb based perovskites can be applied for other combinations of transition metal ions with and without e_g electrons. Indeed we have succeeded in synthesizing Bi_2CoMnO_6 . It was found to be ferromagnets with a T_{CM} of 95 K.

4. CONCLUSION

We have studied the structure and properties of Bi,Pb-3d transition metals perovskites stabilized by high-pressure synthesis. The followings were clarified. $BiCrO_3$ is an antiferromagnetic ferroelectric with $BiMnO_3$ type structure, $BiCoO_3$ and $PbVO_3$ were found to have tetragonal $PbTiO_3$ type structures with large polarizations of $\sim 100 \mu C/cm^2$, $BiNiO_3$ crystallizes in a triclinic structure where disproportionation into Bi^{3+} and Bi^{5+} takes place. Based on these results, new ferromagnetic ferroelectric compound Bi_2NiMnO_6 was designed and was synthesized at 6 GPa

References

- [1] T. Kimura *et al.*, *Nature* **426**, 55 (2003).
- [2] N. Hur *et al.*, *Nature* **429**, 392 (2004).
- [3] R. Seshadri, N. Hill, *Chem. Mater.* **13**, 2892 (2001).
- [4] T. Kuroiwa *et al.*, *Phys. Rev. Lett.* **87**, 217601 (2001).
- [5] G. A. Smolenskii, I. Chupis, *Sov. Phys. Usp.* **25**, 475 (1982).
- [6] J. Wang *et al.*, *Science* **299**, 1719 (2003).
- [7] F. Sugawara *et al.*, *J. Phys. Soc. Jpn.* **25**, 1553 (1968).
- [8] Yu. Ya. Tomashpol'skii *et al.*, *Sov. Phys. - Crystallogr.* **13**, 859 (1969).
- [9] W. L. Roth, R. C. DeVries, *J. Appl. Phys.*, **38**, 951 (1967).
- [10] T. Atou, H. Chiba, K. Ohoyama, Y. Yamaguchi and Y. Syono, *J. Solid State Chem.* **145**, 639 (1999).
- [11] A. Moreira dos Santos, A.K. Cheetham, T. Atou, Y. Syono, Y. Yamaguchi, K. Ohoyama, H. Chiba and C.N.R. Rao., *Phys. Rev. B* **66**, 064425 (2002).
- [12] T. Kimura, *et al.*, *Phys. Rev. B* **67**, 180401(R) (2003).
- [13] S. Niitaka, M. Azuma, M. Takano, E. Nishibori, M. Takata and M. Sakata, *Solid State Ionics* **172**, 557 (2004).
- [14] S. Niitaka *et al.*, *Meeting Abstracts of the Physical Society of Japan, 59th Annual Meeting, Kyushu University, March 27-30, 2004*; **59**, Issue 1, Part 3 (ISSN 1342-8349), 511 (2004).
- [15] A. A. Belik *et al.*, *Chem. Mater.*, in press.
- [16] S. Ishiwata *et al.*, *J. Mater. Chem.* **12**, 3733 (2002).
- [17] A.A. Belik, M. Azuma, T. Saito, Y. Shimakawa and M. Takano, *Chem. Mater.* **17**, 269 (2005).
- [18] M. Azuma, K. Takata, T. Saito, S. Ishiwata, Y. Shimakawa and M. Takano, *J. Am. Chem. Soc.*, **127**, 8889 (2005).
- [19] F. Izumi and T. Ikeda, *Mater. Sci. Forum* **321-323**, 198 (2000).
- [20] S. Niitaka *et al.*, unpublished.
- [21] R. V. Shpanchenko, V. V. Chernaya, A. A. Tsirlin, P. S. Chizhov, D. E. Sklovsky, E. V. Antipov, E P. Khlybov, V. Pomjakushin, A. M. Balagurov, J. E. Medvedeva, E. E. Kaul, C. Geibel, *Chem. Mater.*, **16**, 3267 (2004)
- [22] I. D. Brown, D. Altermatt, *Acta Crystallogr. Sect. B* **41**, 244 (1985).
- [23] S. Ishiwata, M. Azuma, M. Hanawa, Y. Moritomo, Y. Ohishi, K. Kato, M. Takata, E. Nishibori, M. Sakata, I. Terasaki and M. Takano, *Phys. Rev. B*, **72**, 045104 (2005).
- [24] H. Wadati, M. Takizawa, T.T. Tran, K. Tanaka, T. Mizokawa, A. Fujimori, A. Chikamatsu, H. Kumigashira, M. Oshima, S. Ishiwata, M. Azuma and M. Takano, *Phys. Rev. B*, **72**, 155103 (2005).
- [25] C. L. Bull, D. Gleeson, K. S. Knight, *J. Phys.: Condens. Matter*, **15**, 4927 (2003).

(Received December 10, 2005; Accepted January 31, 2006)